Proceedings of the ASME 2010 3rd Joint US-European Fluids Engineering Summer Meeting and 8th International Conference on Nanochannels, Microchannels, and Minichannels
FEDSM-ICNMM2010
August 1-5, 2010, Montreal, Canada

FEDSM-ICNMM2010-30756

FORCES ON BENDS AND T-JOINTS DUE TO MULTIPHASE FLOW

S.P.C. Belfroid
TNO Science and Industry
Delft, The Netherlands
Stefan.Belfroid@tno.nl

M. F. Cargnelutti
TNO Science and Industry
Delft, The Netherlands
Marcos.Cargnelutti@tno.nl

W. Schiferli
TNO Science and Industry
Delft, The Netherlands
Wouter.Schiferli@tno.nl

Marlies van Osch
TNO Science and Industry
Delft, The Netherlands
Marlies.vanOsch@tno.nl

ABSTRACT

To be able to assess the mechanical integrity of piping structures for loading to multiphase flow conditions, air-water experiments were carried out in a horizontal 1" pipe system. Forces and accelerations were measured on a number of bends and T-joint configurations for a wide range of operating conditions. Five different configurations were measured: a baseline case consisting of a straight pipe only, a sharp edged bend, a large radius bend, a symmetric T-joint and a T-joint with one of the arms closed off.

The gas flow was varied from a superficial velocity of 0.1 to 30 m/s and the liquid flow was varied from 0.05 to 2 m/s. This operating range ensures that the experiment encompasses all possible flow regimes.

The magnitude of the measured forces was found to vary over a wide range depending on the flow regime. For slug flow conditions very high force levels were measured, up to 4 orders of magnitude higher than in single phase flow for comparable velocities. The annular flow regime resulted in the (relative) lowest forces, although the absolute amplitude is of the same order as in the case of slug flow.

In case of slug flow, the measured results can be described assuming a simple slug unit model. For both the frequency and amplitude the available models can be used in assessments. In annular and stratified flow a different model is required, since no slug unit is present. Instead, the amplitude of the excitation force can be estimated using mixture properties. To predict the main frequency for the annular flow and stratified flow additional experiments are required.

INTRODUCTION

In many industrial assets is multiphase flow a liability for the mechanical integrity. Typical examples are rapidly accelerating slugs originating in risers, mist flow at high velocity after flash valves or slugs originating from start-up. In all these cases a multiphase flow mixture travels at high velocity through piping systems, including pipe elements such as elbows, T-joints and vessel nozzles (Figure 1, Figure 2). At these elements large dynamic forces are exerted on the pipes due to the large variations in velocity and density. To analyze the integrity of piping systems, estimation models for the amplitude and frequency content of these forces are required. To that end experiments have been set-up to measure the forces on different pipe elements. In this paper the results are discussed and compared to the, sparse available, literature data [1, 2, 3].

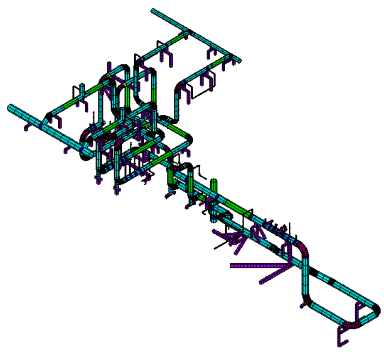

Figure 1: Complex piping system.

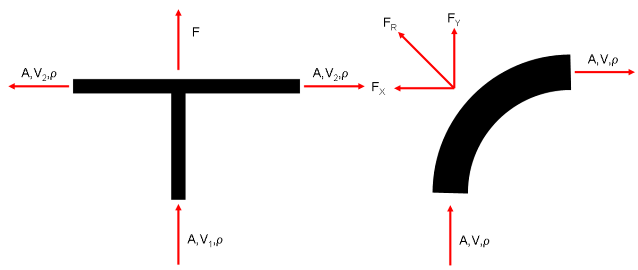

Figure 2: Forces on pipe elements.

EXPERIMENTS AND EXPERIMENTAL SETUP

The experimental setup consists of a perspex pipe with a length of 2600mm and an internal diameter of one inch (254 mm). The air is provided by a central compression system. The liquid used is ultra pure water. The maximum (superficial) flow velocity for the gas is u_{sg}=70 m/s and for the liquid u_{sl}=3 m/s. The complete experimental data map is given in Figure 3 in which all data points are plotted and compared to the classic flow maps.

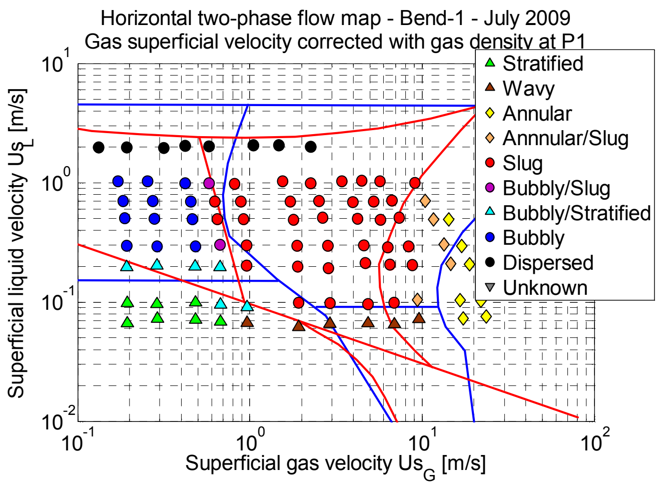

Figure 3: Flow regime map based on visual observations. The red lines indicate the classic flowmap according to Baker [5], the blue lines indicate the flowmap according to Mandhane [4].

The mixing of the two fluids occurs in a y-piece (Figure 4), with the air coming from above. The outlet is a large separator vessel. The pipes (straight pipe, bends or T-joint) are attached to the separator using a flexible hose.

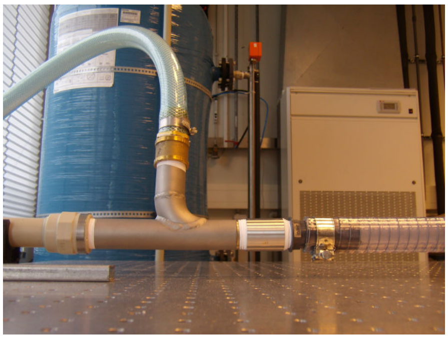

Figure 4: Water-air mixing point.

Figure 5 presents a schematic overview of the test rig, showing the location of the pressure, force and optical sensors. Typically, four dynamic pressure transducers (Kulite XCE-093, HBM P3MB) were used to measure pressure fluctuations. Three of these were placed upstream of the bend, to determine the pressure drop and in particular the slug characteristics such as frequency and velocity. The fourth sensor was placed downstream of the bend and was used to calculate the pressure drop across the bend. Two force sensors (B&K 8302 sn: 10187) were situated at the bend. One upstream and one downstream, both perpendicular to the tube.

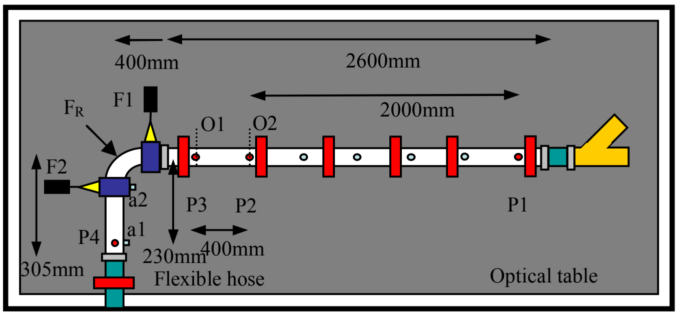

Figure 5: Schematic overview of the experimental setup.

Figure 6 presents the location of the force sensors for both the bend and the T-joint experiments. The force sensors were zeroed at no-flow conditions. Optical sensors (Thor Kabs inc. PPDA/LSD1) were used to detect whether liquid or gas was present in the tube. These were simple light emitters and light sensors which allowed for detection of slugs. However, high gas content slugs proved to be difficult to measure. Finally, a high speed camera (DEWE-CAM-01) was used to film the flow approaching the bend. All measurements were recorded using a Dewetron data acquisition system. This allowed for direct simultaneous recording of all signals including the camera.

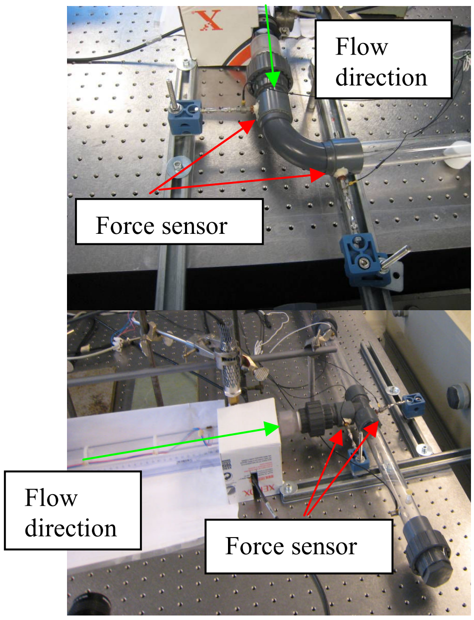

Figure 6: Setup of force transducers.

Five geometries were tested: a single straight pipe, two different bends (named Bend1 and Bend2), one T-joint and one T-joint in which one of the legs was closed off (named T-bend) (Figure 7). The leg was closed off with a leg remaining of 345mm.

In the experiments the measured force was affected by the mechanical response of the complete system, consisting of the tube and the support clamps. The supports were positioned sufficiently far from the bend, that no effect on the forces could be measured. Using a Teflon block to support the bend in the tubing allowed for relatively free movement in the horizontal plane while limiting vertical displacement. In the non flowing situation, the natural eigenmode was approximately 16Hz. This means that for the force measurement results, frequencies below that frequency can be considered to be the directly be from the flow. For near the resonance frequency and higher frequencies the transfer function from the mechanics dominates the result. Of course the 16Hz was determined with an empty tube and with a filled tube the natural frequency will be lower.

In the results of the force measurements, a resulting force F_R (see Figure 5) is presented. This force, for the bend experiments (Bend1, Bend2 and T-bend), is given by:

$$F_R = \sqrt{F_1^2 + F_2^2} \quad (1)$$

For the T-joint this resulting force is given by:

$$F_R = \sqrt{F_1^2} \quad (2)$$

Figure 7: Three test geometries (Top: Bend1, Middle right: Bend2, bottom T-Joint).

EXPERIMENTAL RESULTS

The goal of the experiments is to determine models for both the frequency and the amplitude of the forces exerted on the piping system.

FREQUENCY

In Figure 8 a typical frequency spectrum for slug flow is given. The frequency spectrum for the slug flow shows a clear peak, corresponding to the slug frequency. This clear peak is less pronounced for the other flow regimes.

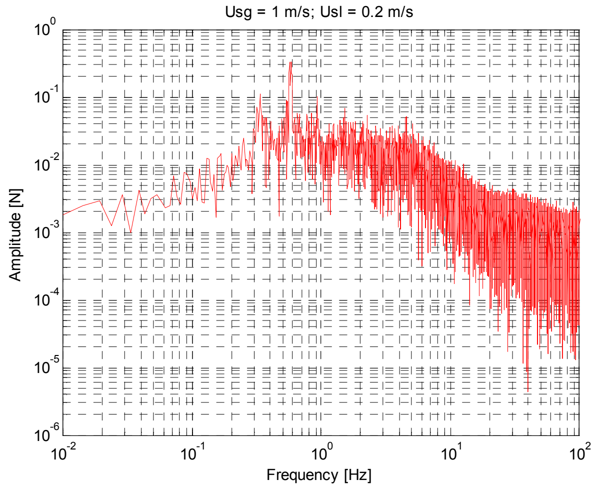

Figure 8: Frequency spectrum for a characteristic measurement (F1, Bend1).

In Figure 9, the frequency spectra are plotted for four flow regimes: slug flow, annular flow, stratified flow and single phase gas flow. The spectra have been normalised with the maximum amplitude. The slug flow spectrum has a clear peak at low frequency (≈0.6Hz) corresponding to the slug frequency. The annular flow regime shows a more broadband spectrum with also energy present at higher frequencies. The stratified flow spectrum is much more complex with several peaks. These peaks could be due to acoustic and mechanical resonances in the system. For the single phase the spectrum is a very broadband signal with a large low frequency component.

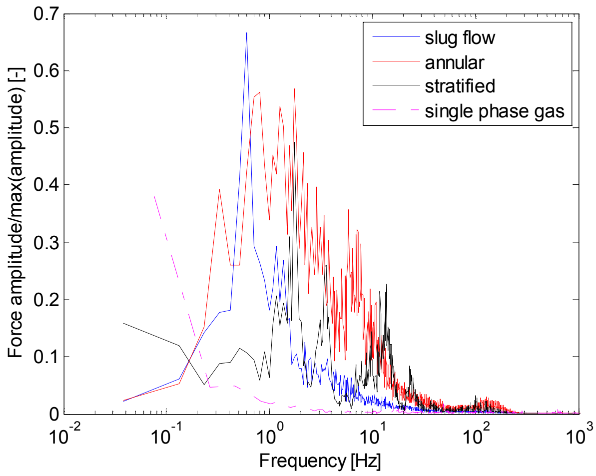

Figure 9: Frequency spectrum for four flow regimes: Slug flow (u_{sg}=3m/s, u_{sl}=0.3m/s), annular flow (u_{sg}=30m/s, u_{sl}=0.07m/s), stratified flow (u_{sg}=0.2m/s, u_{sl}=0.07m/s) and single phase gas flow (u_{sg}=3m/s, u_{sl}=0.0m/s). All for sensor F1 for the experiments with Bend 1.

The slug frequency (f_{slug}) is determined by peak count in the optical signals and the pressure signals. In Figure 10, the results are compared to a model by Fetter [6]. This model corresponds well with other classical models such as Manolis [7] and Heywood and Richardson [8]. This model gives the slug frequency as:

$$f_{slug} = 0.0175 \cdot Fr_{Fet}^{1.37} \tag{3}$$

with the Fetter slug frequency Froude number defined as:

$$Fr_{Fet} = \frac{u_{s,l}}{gD}\left(\frac{21.3+u_m^2}{u_m}\right) \tag{4}$$

The agreement is very good for the lower gas velocities. Similar to the slug velocity, for the higher gas velocities there is not a good agreement between the frequency measurements and the Fetter model. Instead of an increase, the frequency decreases. The reason for this behaviour could be that for the higher gas velocities the length of the tube is not long enough and the slugs are still accelerating and they are not yet fully developed.

The frequency can also be expressed as a Strouhal number. The Strouhal number is defined as:

$$Sr = \frac{fD}{u_{sl}} \tag{5}$$

In Figure 11, the Strouhal number is plotted as function of the no-slip liquid hold-up for the current experiments and for literature data for different tube diameters. The hold-up is a measure for the liquid content. The current measurement results are in fair agreement with the other literature data.

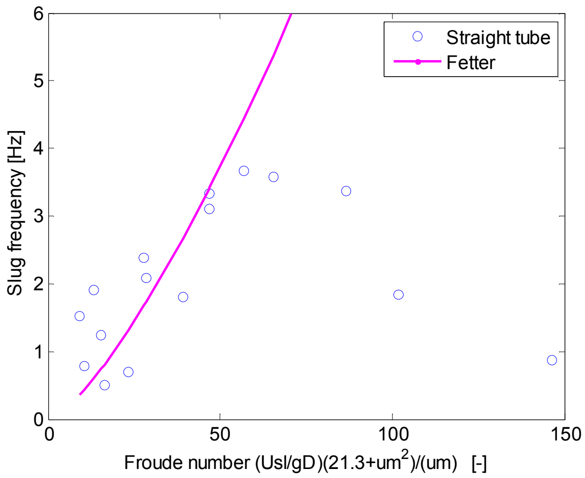

Figure 10: Slug frequency as function of Fetter slug Froude number.

This means that the slug frequency can be described reasonably well. The main frequencies for the stratified and annular flow are less defined. For an isotropic turbulence, the results should be centered around a mid frequency of V_c/L_{turb} , with V_c the convective speed of the energy carrying eddies and L_{turb} [10]. For single phase flow the size of the eddies is approximately $0.1D_{tube}$. With a convective speed corresponding to the mean velocity this would mean a typical centre frequency 12 kHz (for the annular flow case as plotted in Figure 9). If the friction velocity is taken as more representative of the convective velocity the centre frequency is still 530Hz. The second main frequency is determined by the wave velocity. The wave frequency is in the order of $Sr=f_{wave}D_{tube}/u_{sG}= 0.01$ [11]. This gives frequencies of 10Hz. This seems comparable to our measurements although the central peak frequency of most of the annular flow cases seems lower than Sr=0.01. The reason for the difference must be analyzed yet. Of course, due to the nature of the experiments, the transfer of the mechanical structure always plays a role, although the frequencies measured are lower than the, empty tube, natural frequency of the set-up around the bend.

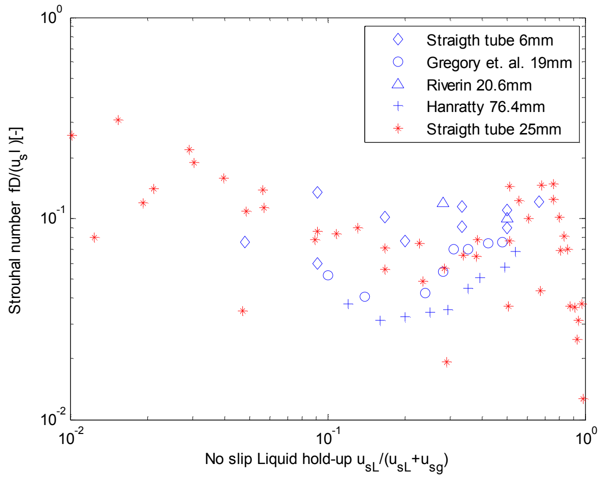

Figure 11: Strouhal number as function of no slip liquid hold-up. Comparison with results from Cargnelutti [3], Riverin [1], Gregory and Hanratty [9].

AMPLITUDE

In Figure 12 the results for the Bend1 experiments are plotted as function of the mixture velocity. It is clear that multiphase flow conditions have a much larger dynamic force compared to the single phase experiments. The highest forces are measured for the slug flow regime. However, the absolute forces exerted in the annular flow regime can be nearly as large as force the slug flow regime due to the higher velocities occurring in that regime. Only for the stratified flow the forces are low for almost all flow rates.

One of the main reasons for the flow regime dependency is the liquid content. Due to its high density, liquid carries much more momentum than gas travelling at similar velocities. Therefore, the momentum change in the bend is much larger for liquid than for gas. This can be properly seen in Figure 13, in which the dimensionless force is plotted as a function of the no-slip liquid hold-up. For lower liquid content the, dimensionless, forces reduces fast, because the mass of the flow reduces rapidly. Also at near-liquid conditions, the dimensionless force reduces. This is caused by the fact that the high hold-up cases occur only at low velocities and the dynamic forces reduce for those low velocities. Surprisingly, there is quite a large spread for the single phase liquid cases. The cases for which the single phase, dimensionless, liquid forces are higher than the trend for the multiphase cases are those with low liquid velocities and therefore also very low absolute forces. The force measurements might be not representative for those low values. The effect of the mass of the fluid can also be seen if instead of using the liquid momentum the mixture momentum is used to make the forces dimensionless (Figure 14). The dimensionless force is almost constant (at approximately 5) across a large range of liquid hold-up.

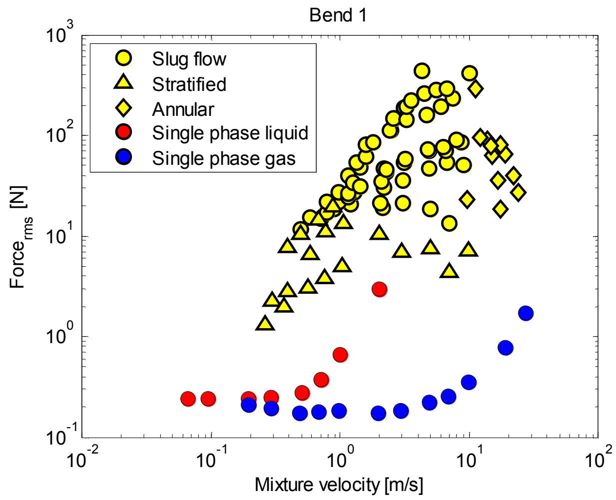

Figure 12: Force (rms) as function of the mixture velocity differentiated between slug flow (yellow circles), stratified flow (yellow triangles), annular flow (yellow diamonds), single phase gas (blue circles) and single phase liquid (red circles) for Bend1 experiments.

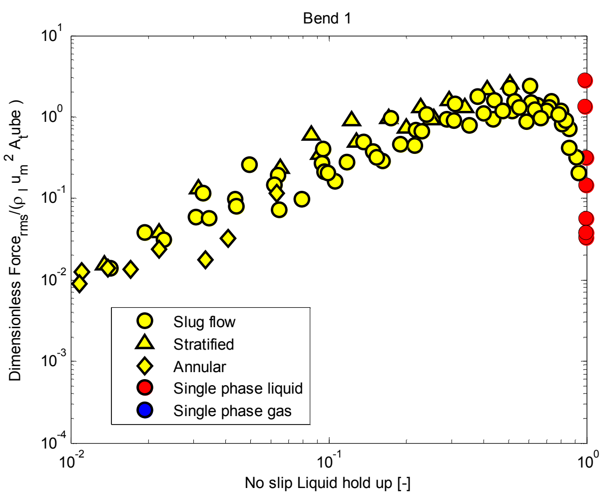

Figure 13: Force (rms), made dimensionless with the liquid momentum, as function of the no slip liquid hold-up differentiated between slug flow (yellow circles), stratified flow (yellow triangles), annular flow (yellow diamonds), single phase gas (blue circles) and single phase liquid (red circles) for Bend1 experiments.

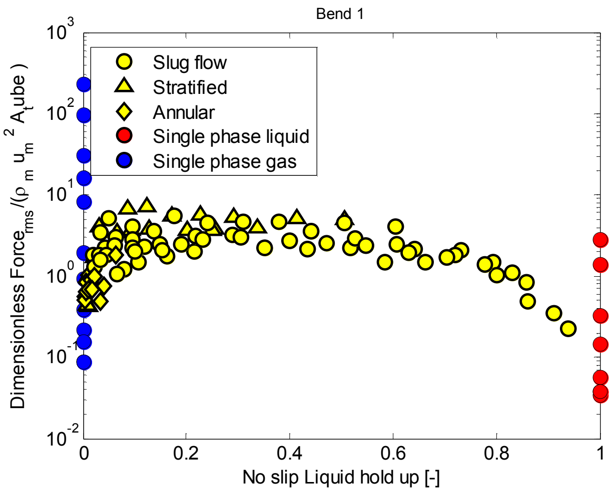

Figure 14: Force (rms), made dimensionless with the mixture momentum, as function of the no slip liquid hold-up differentiated between slug flow (yellow circles), stratified flow (yellow triangles), annular flow (yellow diamonds), single phase gas (blue circles) and single phase liquid (red circles) for Bend1 experiments.

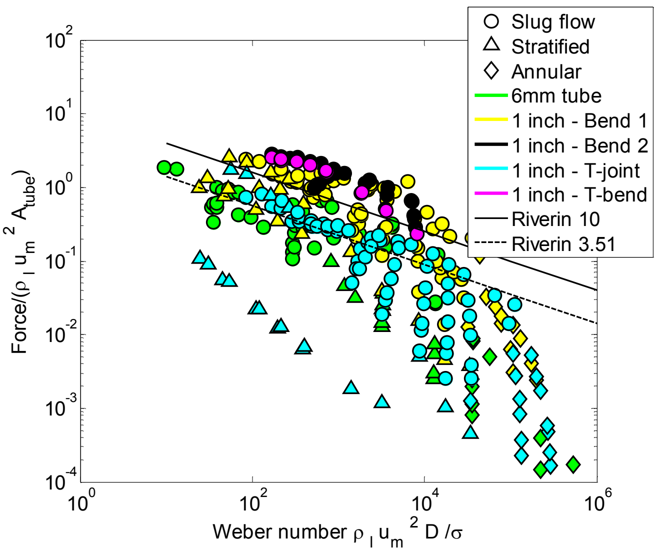

Figure 15: Dimensionless force as function of Weber number.

In Figure 15 the dimensionless force is plotted as function of the Weber number for all geometries. For comparison, results of measurements on a scale of 6 mm [3] have been added as well as the the relationship proposed by Riverin [1]. The relationship is plotted with different values for the constant (C) proposed by Riverin:

$$\overline{F_{rms}} = \frac{F_{rms}}{\rho_l u_m^2 A} = CWe^{-0.4} \tag{6}$$

Two values for C are plotted: C=10, as used by Riverin for his data set and C=3.51, which is the best fit with the slug flow experiments for the 6mm experiments. From this comparison several observations can be made:

- The results for Bend1 and Bend2 are very comparable. This could be due to the fact that the slug length was typically larger than the bend radius.
- The results for the T-joint are lower than the Bend experiments. This can be explained from the fact that the flow is symmetrically splitted in two. This results in lower forces. The axial forces (sensor F2) are about twice the force in the perpendicular directin (sensor F1).
- The results for the T-bend are comparable to the Bend experiments. In practice the closed leg filled almost completely with liquid and a sharp bend is formed in that case.
- The forces in the 6 mm scale were slightly lower than for the 1 inch experiments. This was unexpected as the slugs in the 1 inch scale experiments contain more gas than for the smaller scale. The difference could be due to the stiffness of the material (glass vs. perspex).
- The current experiments show higher forces also compared to the Riverin experiments.

MECHANICAL ASSESSMENT

For an integrity assessment both the amplitude and frequency on the pipe elements are required. For the slug a fully separated slug flow with a given slug flow velocity and slug frequency is assumed. For the slug velocity models like Collins [12] can be used and for the slug frequency the model of Fetter is recommended. In that way slug propagation through the piping system can be tracked (Figure 16) and the force as function of time can be calculated assuming that the dynamic force is solely due to a change in momentum direction [3].

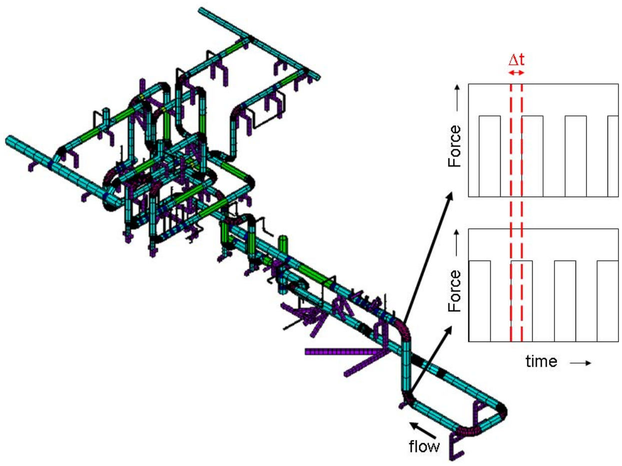

Figure 16: Slug propagation through the piping system.

For the annular flow, a mixture model approach is recommended for the forces amplitude. In this, the force is based on the mixture density and the mixture velocity. The resulting force is compared to the measurements in Figure 17 for both the slug and the mixture approach. The approaches for the slug and annular flow regime give an estimate useable in screening assessments. Only for the frequency spectrum for annular flow, a larger uncertainty must be taken, as for this regime the required models are not general enough.

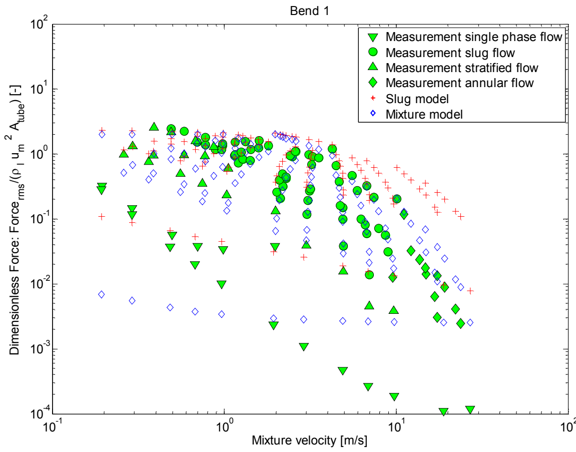

Figure 17: Dimensionless force as function of mixture velocity.

CONCLUSIONS

The flow characteristics of an air-water flow through 1 inch tubes have been analyzed. The flow regime map corresponds well with the classic flow maps. Measured forces vary significantly depending on flow regime. The highest force levels are observed in the slug flow regime, whereas stratified flow gives the lowest force levels. The forces decrease roughly linearly with the liquid content. The force amplitude was measured to be between 1 and 10 times the liquid momentum based on the mixture velocity. A comparison showed higher force values that those reported by Riverin.

No effect of bend radius was found. Three bends were measured (a sharp edged bend, a large bend radius bend and a bend with a closed side branch), and all results were comparable. The results for a real T-joint were significantly lower than for the bends.

In case of slug flow, the measured results can be described assuming a simple slug unit model. Both the amplitude and frequency can be described well with this method. In annular and stratified flow a different model is required, since no slug unit is present. Instead, excitation force can be estimated using mixture properties. This mixture approach also describes the forces for the slug regime relatively well. To model the centre frequency of the force spectrum in case of the annular flow regime requires additional investigations.

NOMENCLATURE

A	Tube cross sectional area	[m^2]
C	Force proportionally factor	[-]
D	Tube diameter	[m]
F_{rFet}	Fetter slug frequency Froude number	[-]
F_{rg}	Froude gas number	[-]
F_{rl}	Froude liquid number	[-]
F_{rms}	RMS value of F_R	[N]
F_{std}	Standard deviation of F_R	[N]
Sr	Strouhal number	[-]

We	Weber number	[-]
f_{slug}	Slug frequency	[Hz]
g	Gravitational acceleration	[m/s^2]
u_m	Mixture velocity	[m/s]
$u_{s,g}$	Superficial gas velocity	[m/s]
$u_{s,l}$	Superficial liquid velocity	[m/s]
α_l	Liquid hold-up	[-]
ρ_l	Liquid density	[kg/m^3]
ρ_m	Mixture density	[kg/m^3]
σ	Surface tension	[N/m]

ACKNOWLEDGMENTS

The authors are grateful that the ISAPP consortium (Shell, Delft Technical University, TNO) allowed the publication of this work..

REFERENCES

[1] Riverin, J.L., De Langre, E., Pettigrew, M.J., 2006, "Fluctuating forces caused by internal two-phase flow on bends and tees", JSV 298, pp. 1088-1098.

[2] Tay, B.L. and Thorpe, R.B., 2004, "Effects of Liquid Physical Properties on the Forces Acting on a Pipe Bend in Gas–Liquid Slug Flow", Chemical Engineering Research and Design, 82(3), pp. 344-356.

[3] Cargnelutti M.F., e.a, "Two-phase flow-induced forces on bends in small scale tubes", PVP2009-77708, 2009 ASME Pressure Vessels and Piping Division Conference, Prague, 2009

[4] Mandhane, J.M., Gregory, G.A., and Aziz, K., 1974, "A Flow Pattern Map for Gas-Liquid Flow in Horizontal Pipes", Int. J. Multiphase Flow, 1(4), pp. 537-553.

[5] Chiaasiaan S.M. , "Two-phase Flow, boiling, and condensation" (1st edition, 2008)

[6] Fetter, C.P., 1988, "Development of a Clamp-on Acoustic Two-Phase Flow Meter", M.Sc. thesis, TUDelft, Netherlands.

[7] Manolis, I.G., 1995, "High pressure gas–liquid slug flow", Ph.D. Thesis, Imperial College, London, UK.

[8] Heywood, N.I. and Richardson, J.F., 1979, "Slug flow of air–water mixtures in a horizontal pipe: Determination of liquid hold-up by γ-ray absorption", Chem. Eng. Sci. 34, pp. 17–30.

[9] Woods, B.D., Fan, Z., Hanratty, T.J., 2006, "Frequency and development of slugs in a horizontal pipe at large liquid flows", IJMP, 32(8), pp. 902-925.

[10] E. Naudasher, D. Rockwell, "Flow-Induced Vibrations. An Engineering Guide" (2005)

[11] D. Schrubing, T.A. Shedd, "Two-phase wavy-annular flow in small tubes", IJHMT 52 (2009) 1619-1622

[12] Collins, R., de Moraes, F.F., Davison, J.F. and Harrison, D., 1978, "The motion of a large gas bubble rising through liquid flowing in a tube", J. Fluid Mech., 89, pp. 497-514.

